

S-DES: Detached Eddy Simulation coupled with steady RANS in the wall region

Lars Davidson, Chalmers University of Technology, Gothenburg, Sweden

Introduction

Xiao *et al.* [1] proposed an interesting hybrid LES/RANS method in which they solve the RANS and LES equations in the entire computational domain. They couple the two solutions through drift terms. Near walls, drift terms are added to the LES equations so that the time filtered LES quantities (velocity, modeled turbulent quantities) agree with the time filtered RANS quantities. Away from the walls, drift terms are added to the RANS equations so that the time-filtered RANS quantities agree with the time-filtered LES quantities. In the present work this method is simplified and used as a hybrid RANS-LES method, a *wall-modeled* DES. The new method is called **S-DES**.

The Hybrid S-RANS/LES methodology

The domain is split into a steady RANS region (S-RANS) and LES region (LES), see Fig. 1a. Two sets of equations (steady RANS and unsteady DES) are solved in the entire domain on identical grids although the S-RANS mesh may be two dimensional (as in the present work). Drift terms are added

- in the LES equations, S_i^{LES} , in the S-RANS region and
- in the RANS equations, S_i^{RANS} , in the LES region

which read

$$S_i^{LES} = \frac{v_i^{RANS} - \langle \bar{v}_i^{LES} \rangle_T}{\Delta t}, \quad S_i^{RANS} = \frac{\langle v_i^{LES} \rangle_T - v_i^{RANS}}{\Delta t} \quad (1)$$

Subscript T indicates integration over time T

$$\langle \phi(t) \rangle_T = \frac{1}{T} \int_{-\infty}^t \phi(\tau) \exp(-(t-\tau)/T) d\tau \Rightarrow \langle \phi \rangle_T^t \equiv \langle \phi \rangle_T = a \langle \phi \rangle_T^{t-\Delta t} + (1-a) \phi^t \quad (2)$$

where $a = \exp(-\Delta t/T)$. Note that although the flow cases include homogeneous direction, no space averaging is made in Eq. 2.

The present method is similar to those in [1–3]. The main differences are that

- in [1, 3] they use two drift terms in the LES momentum equations to ensure that the resolved Reynolds stresses are equal (similar) to the modeled ones in the RANS equations. Here we use only one. They include drift terms also in the k and ε equations [1] or the k equation [3].
- in [1, 3] they include tuning constants in all drift terms. Here we use no tuning constant.

The $k - \omega$ Model

The Wilcox $k - \omega$ turbulence model is used in both the LES and RANS regions.

$$\begin{aligned} \frac{\partial k}{\partial t} + \frac{\partial \bar{v}_i k}{\partial x_i} &= P^k - \frac{k^{3/2}}{\ell_t} + \frac{\partial}{\partial x_j} \left[\left(\nu + \frac{\nu_t}{\sigma_k} \right) \frac{\partial k}{\partial x_j} \right] \\ \frac{\partial \omega}{\partial t} + \frac{\partial \bar{v}_i \omega}{\partial x_i} &= C_{\omega_1} \frac{\omega}{k} P^k - C_{\omega_2} \omega^2 + \frac{\partial}{\partial x_j} \left[\left(\nu + \frac{\nu_t}{\sigma_\omega} \right) \frac{\partial \omega}{\partial x_j} \right] \end{aligned} \quad (3)$$

The DES $k - \omega$ Model

The DES equations are solved in the entire region, but they govern the flow only in the LES region, see Fig. 1a. In the RANS regions, the lengthscale in Eq. 3 is computed as $\ell_t = k^{1/2}/(C_\mu \omega)$ and in the LES region it is taken from the IDDES model [4], i.e.

$$\ell_t = C_{LES} \Delta_{dw}, \quad \Delta_{max} = \max\{\Delta x, \Delta y, \Delta z\}, \quad \Delta_{dw} = \min(\max[C_{dw} d_w, C_w \Delta_{max}, \Delta_{nstep}], \Delta_{max}) \quad (4)$$

The RANS $k - \omega$ EARSM Model

The steady RANS equations are solved in the entire region, but they govern the flow only in the RANS region, see Fig. 1a. The Reynolds stresses, $\overline{v_i' v_j'}$, are computed from the two-dimensional algebraic Reynolds stress model (EARSM) [5]

Numerical procedure

The simulations are initialized as follows:

- The 2D RANS equations are solved
- Anisotropic synthetic fluctuations are superimposed to the 2D RANS field which gives the initial LES velocity field. The initial $\langle v_i^{LES} \rangle_T$ is set from the 2D RANS field.

The RANS solver is called every 10th timestep which means that the additional computing time is negligible.

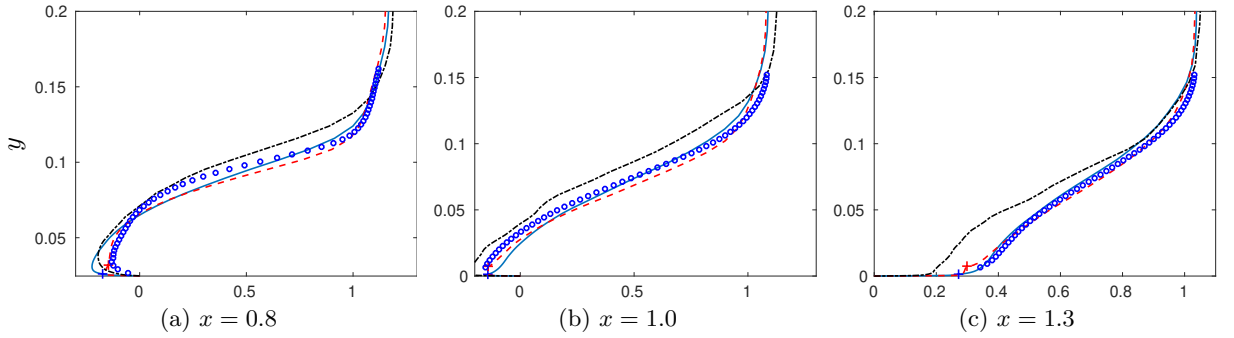
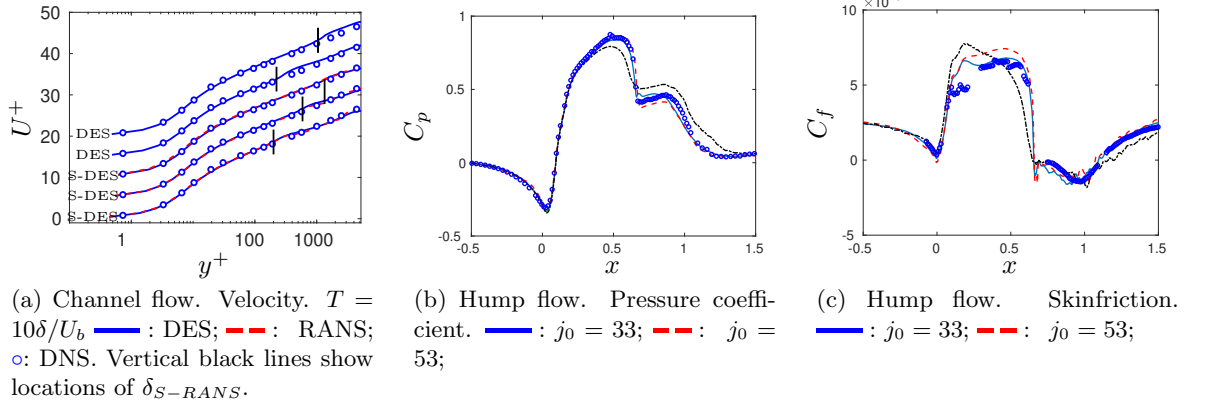
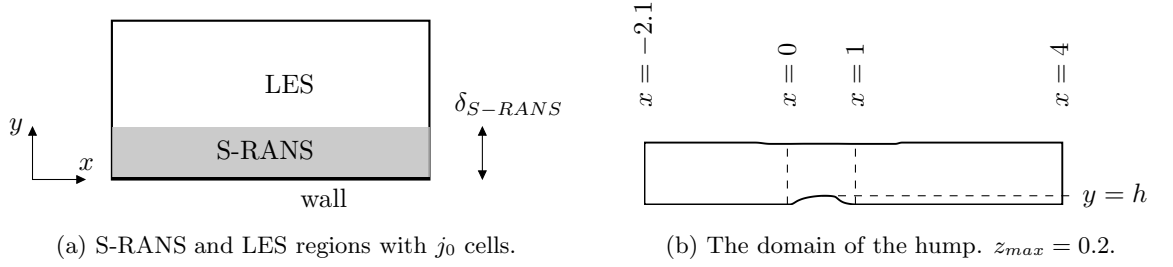


Figure 3: Hump flow. $T = 20h/U_b$. $\langle \bar{v}_1 \rangle$ velocities. —: S-DES, $j_0 = 33$; - - : S-DES, $j_0 = 53$; - - - : pure DES; \circ : exp

Results

The first test case is fully developed channel flow with periodic boundary conditions in streamwise (x) and spanwise (z) directions. The Reynolds number, $Re_\tau = u_\tau \delta / \nu$, is 5200 where δ denotes half-channel width. The size of the domain is $x_{max} = 3.2$, $y_{max} = 2$ and $z_{max} = 1.6$. The mesh has $32 \times 96 \times 32$ (x, y, z) cells. Figure 2a shows the velocity profiles for S-DES for three locations of δ_{S-RANS} and pure DES simulations for two locations of δ_{S-RANS} . The three S-DES give no log-law mismatch whereas the two pure DES give a small log-law mismatch.

The second test case is the flow over a two-dimensional hump, see Fig. 1b. The Reynolds number of the hump flow is $Re_c = 936000$. The mesh has $386 \times 120 \times 32$ cells (x, y, z) and it is taken from the NASA workshop.¹ The inlet is located at $x = -2.1$ and the outlet at $x = 4.0$, see Fig. 1b.

The inlet profiles are taken from a separate 2D RANS simulation with the same momentum thickness as the experimental velocity profiles. Anisotropic synthetic fluctuations are superimposed to the inlet velocity profile. Periodic boundary conditions are used in the spanwise direction (z). The interface between the S-RANS domain and the LES domain is defined along a gridline. Two different locations of δ_{S-RANS} are evaluated below: $j_0 = 33$ and 53 which correspond to $y^+ = 50$ and 250, respectively, at the inlet. The integration time-scale is set to $T = 20\delta/U_b$. Some results are presented in Figs. 2b, 2c and 3. As can be seen, the agreement with experiments is good for S-DES much not so good for pure DES. The integration time, T , for S-DES is close to the minimum value ($T = 5$ is too low).

In the full paper the strengths and weaknesses of the model will be analyzed.

¹https://turbmodels.larc.nasa.gov/nasahump_val.html

References

- [1] H. Xiao and P. Jenna. *Journal of Computational Physics*, 231:1848–1865, 2012.
- [2] B. de Laage de Meux, B. Audebert, R. Manceau, and R. Perrin. *Physics of Fluids A*, 27(035115), 2015.
- [3] R. Tunstall, D. Laurence, R. Prosser, and A. Skillen. *Computers & Fluids*, 157:73–83, 2017.
- [4] M. L. Shur, P. R. Spalart, M. Kh. Strelets, and A. K. Travin. *International Journal of Heat and Fluid Flow*, 29:1638–1649, 2008.
- [5] S. Wallin and A. V. Johansson. *Journal of Fluid Mechanics*, 403:89–132, 2000.